Proceedings of the 4th WSEAS/IASME Int. Conf. on System Science and Simulation in Engineering, Tenerife, Spain, December 16-18, 2005 (pp186-191)

# Design and Laboratory Tests of Wheeled Mobile Robots

**Yaser Maddahi**
Mechanical Engineering Department
Islamic Azad University (Saveh Branch)
Robotic and Automation Research Laboratory, Engineering Department, Islamic Azad University (Saveh Branch), Saveh
IRAN

*Abstract:* One of the major tasks of autonomous robot navigation elimination of robot errors. These errors are caused by imperfections in the design and mechanical implementation of robots. This paper presents experimental and statistical analysis of wheeled robots. The mobile robots consist of three differential drive robots that tested and moved in given trajectories and then the systematic errors of the robots are determined. Finally this research is concluded with comparing the results of statistical analysis for robots and some major parameters are defined for validation of the error correction in considered robots.

*Key-Words:* Systematic Error, Mobile Robot, Differential Drive Robot, Experimental Analysis.

## 1 Introduction

In many applications of mobile robots, the systematic errors are occurred because the imperfection in mechanical design. To study the possibilities of testing robots, an experimental robot has designed and constructed.

Considerable research has been performed in the area of systematic error analysis and calibration of robots [1]. Maddahi introduces a new method for measuring the odometry errors in a four-wheeled robot [2]. Sreenivasan has designed articulated wheeled vehicles to eliminate kinematics wheel surface slipping [3]. Hamdy developed a tenth-order nonlinear dynamic model for a wheeled mobile robot [4]. Balakrishna developed a traction model accounting for slip in non-holonomic wheeled mobile robots [5]. Scheding presents experimental evaluation of a navigation system that handles autonomous vehicle wheel slip [6]. Watanabe designed a controller for an autonomous omni-directional mobile robot for service applications [7]. Dickerson and Lapin present a controller for omni-directional Sweden- wheeled vehicles that includes wheel slip detection and compensation [8]. Maddahi and Bani Rostam designed and developed an omni-directional mobile robot with experimental analysis results [9].

This paper covers the overall design processes of differential drive mobile robots. In order to measuring systematic errors, the consequences of experimental tests in given trajectories are carried out. The UMB Mark method is used for determining the errors of differential drive robots.

## 2 Design of Mobile Robots

For designing a robot some factors such as: environment and robot tasks play important roles. In addition other factors such as: weight of robot, type of wheels, material of wheels and rollers and control devices influence in design. Design process starts by knowledge acquisition about robot parts and environment [10].

The construction of differential drive robot is consisting of two drive wheels and two castor wheels, two pulley-belt systems, two shafts that connect the wheels to pulleys, a small driver system with L297 IC and a processor for data processing transmitted to the robot.

By cases hereinafter-described structure of three differential drive mobile robots is considered.

### Case I: Robotest

Robotest consists of two drive wheels with its own stepper that is controlled by a Pentium III computer and two free castor wheels providing the robot stability. The castors cause slipping during direction changes. These parts are shown in manufactured model of the robot in Fig. 1.

### Case II: MoboLab

This robot named MoboLab has dimension of $60 \times 60 \times 20\ cm^3$ and weighs 10 kg. (Fig.2) Mobolab has two drive wheels and two free castor wheels, two stepping motors with a 78/16 spur gears transmission ratio for each motor and a maximum 1 N.m output. The motor shaft rotates $1.8^\circ$ per step.

The rotation can be transformed to a linear movement of wheels that depends on the diameters of the gear and wheels. The diameter of driver wheels is about 100 mm and the width is about 30 mm. The material of wheels is rubber in the contact point with ground. There is a little elastic deformation in the gears.

Fig. 1. Manufactured Robotest (Case I) [11]

The controller computes the command signals from the reference trajectory, processed by the sensory feedback measurement. For these purpose two shaft encoders are used. The controller communicates the command signals to pulse the stepper motor in the robot drive. The robot employs infrared sensor for obstacle avoidance and a 486-laptop computer for control and programming [12].

Fig. 2. Manufactured Mobolab (Case II)

### Case III: Sweeper

This mobile robot is designed and constructed for sweeper robots competition and has two drive wheels, two castor wheels and two stepping motors (1.8 deg/step) with a spur gears transmission ratio. The diameter of drive wheels is about 195 mm and the thickness is about 10 mm. The material of wheels in contact point with ground is a rubber ring. This mobile manipulator has two arms that one of them is fixed to robot and the other rotate around it's joint. Therefore this robot has three degrees of freedom comprising two DOF in base and one DOF in arm (Fig. 3).

A Pentium III, 850 MHz processor is used for path detection algorithm processing. A webcam provides images acquisition from environment. With the data sent by camera, robot is able to detect the objects such as obstacles. This camera obtains environment data and sends it to microcontrollers and processor. After data processing by microprocessor, commands in packets are sent to microcontrollers through serial port, translated and finally transmit them to two stepper motors for moving and three motors for controlling the arms.

Fig. 3. Manufactured Sweeper robot (Case III)

## 3 Experimental Test

Odometry is the measurement of the wheel rotation as a function of time. If the drive wheels of the robot are joined to a common axle, the position and orientation of the axle centre relative to the previous position and orientation can be determined from odometry measurements on all wheels. In experimental tests, incremental encoders are mounted onto drive wheels.

3.1 Investigation of error factors in mobile robot

Systematic errors are usually caused by imperfections in the design and mechanical implementation of a mobile robot and caused by some resources. In differential drive mobile robots, the two most notorious systematic error sources are:

Unequal wheel diameters:

$$E_d = \frac{D_R}{D_L} \tag{1}$$

Uncertainty about the wheel base.

$$E_b = \frac{b_{actual}}{b_{\mathrm{nominal}}} \qquad (2)$$

Where $D_R$, $D_L$ are the actual right and left wheel diameters and $b_{actual}$, $b_{nomizzl}$ is the actual and nominal wheelbase of the robot [13].

3.2 Measurement and correction of systematic odometry errors

One of the methods for measuring odometry errors is benchmark series test which allows the experimenter to draw conclusions about the overall odometric accuracy of the robot and to compare the performance of different mobile robots from different manufacturers. The first benchmark test is called the "uni-directional square path" test [13]. The robot starts out at a position which is labelled START and move on a $4\times4$m uni-directional square path. The robot is programmed to traverse the four legs of the square path but because of odometry and controller errors, not precisely to the starting position. The fact that two different error-mechanisms might result in the same overall error may lead an experimenter toward a serious mistake: correcting only one of the two error sources in software. Simulation of a differential drive mobile robot with two difference odometry error sources shows the effect of errors in robot motion.

To overcome the problems a new method called the "bi-directional square path test" was introduced. In this experiment the robot was programmed to follow a 4×4 m square path in clockwise (cw) and counter-clockwise (ccw) directions.

Upon completion of the square path in each direction, the experimenter again measures the absolute position of the vehicle. Then these absolute measurements are compared to the position and orientation of the vehicle as computed from odometry data.

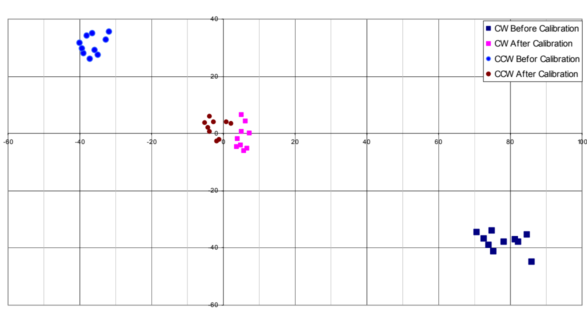


Fig. 4. Results of UMBmark test in cw and ccw directions before and after calibration for robot case I(Robotest)

The coordinates of the two centers of gravity are computed as follow:

$$\mathrm{X}_{\mathrm{c.g,cw/ccw}} = \frac{1}{n}\sum_{i=1}^{n} \varepsilon x_{i,cw/ccw} \qquad (3)$$

$$\mathrm{Y}_{\mathrm{c.g,cw/ccw}} = \frac{1}{n}\sum_{i=1}^{n} \varepsilon y_{i,cw/ccw} \qquad (4)$$

where n = 10 is the number of runs in each direction.

Figure 4 shows experimental results of this method in two cw and ccw directions, before and after calibration in robot case I (Robotest). Also Fig. 4 shows the contribution of two type errors (Type A and Type B). Type A errors are caused mostly by $E_d$. The errors cause too much or little turning at the corners of the square path. The amount of rotational of error in each nominal 90 turn is denoted by $\alpha$ and measured in radian. Type B errors are caused mostly by the ratio between wheel diameters $E_d$ and they cause a slightly curved path instead of a straight one during the four straight legs of the square path. Because of the curved motion, the robot will have gained an incremental orientation error $\beta$, at the end of each straight leg. $\alpha$ and $\beta$ can be found from simple geometric relations.

$$\alpha = \frac{(Xc.g.cw + Xc.g.ccw)}{-4L} \cdot \frac{180}{\pi} \qquad (5)$$

$$\beta = \frac{(Yc.g.cw + Yc.g.ccw)}{-4L} \cdot \frac{180}{\pi} \qquad (6)$$

where L is straight leg of the square path.

Finally, two correction factors can be defined by: [13]

$$C_L = \frac{2}{E_d + 1} \qquad (7)$$

$$C_r = \frac{2}{\frac{1}{E_d} + 1} \qquad (8)$$

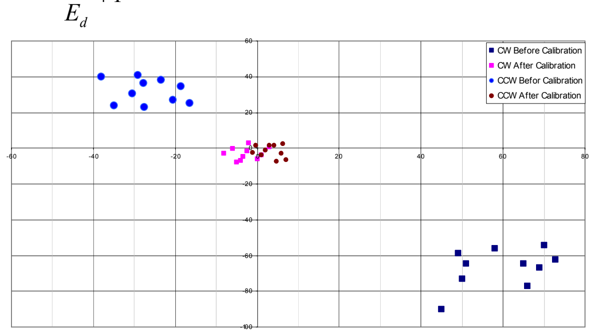


Fig. 5. UMBmark test results in two directions before and after calibration for Mobolab(case II)

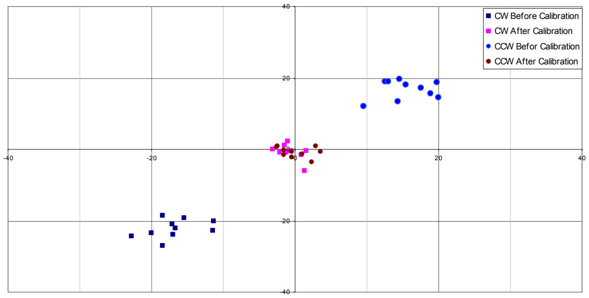


Fig. 6. Results of UMBmark test in two directions before and after calibration for Sweeper (Case III)

Results of test for correcting wheel base and effective wheel diameter ratio errors are presented. These tests performed with described differential drive mobile robots. Figs 6-8 show the results of the uncalibratted runs and calibrated runs in cw and ccw directions for robots.

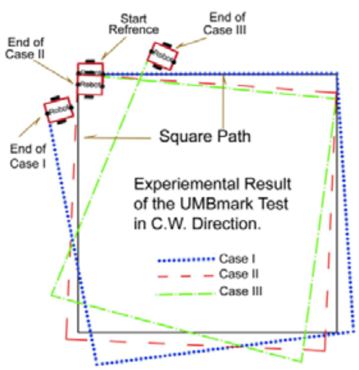


Fig. 7 UMBmark test path in cw direction for differential drive robots case I, II and III

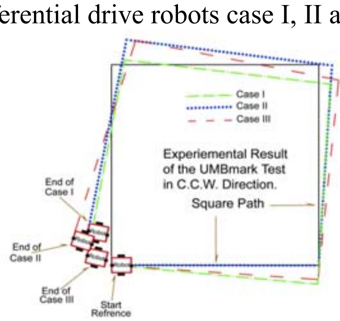


Fig. 8 UMBmark test path in ccw direction for differential drive robots case I, II and III

Figs. 7and 8 show the effect of errors in robot motion in cw and ccw directions. These data obtained from experimental tests and vehicles are shown in average errors.

For comparison between robots operations before and after calibration the end position of robots in cw and ccw directions are presented in Figs 9 to 11. The bars in figures show the final position of robots that calculated by Esq. (9) and (10).

After conducting the UMBmark experiments for minimizing the effect of non systematic errors, suggested to consider the center of odometry errors in cw and ccw directions. The absolute offsets of two centers of gravity are given by:

$$r_{c.g.,c.w.} = \sqrt{\left(x_{c.g.,c.w.}\right)^2 + \left(y_{c.g.,c.w.}\right)^2} \qquad (9)$$

$$r_{c.g.,c.c.w.} = \sqrt{\left(x_{c.g.,c.c.w.}\right)^2 + \left(y_{c.g.,c.c.w.}\right)^2} \qquad (10)$$

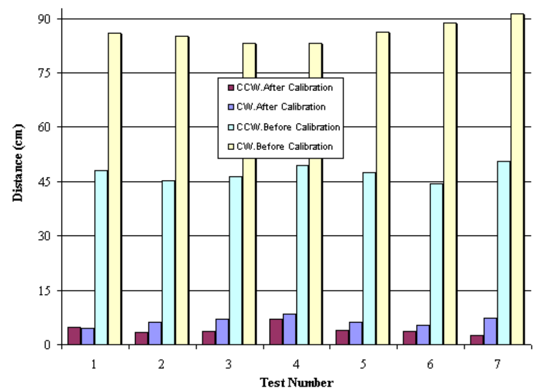


Fig. 9. End position of Robotest motion in cw and ccw direction before and after calibration

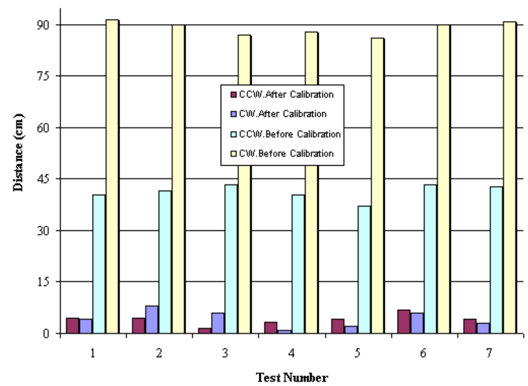


Fig. 10. End position of Mobolab motion in cw and ccw direction before and after calibration

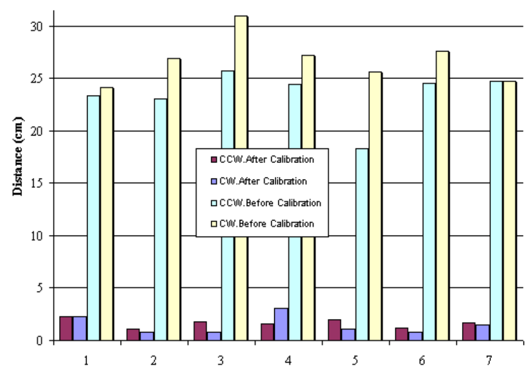


Fig. 11. End position of Sweeper motion in cw and ccw direction before and after calibration

Proceedings of the 4th WSEAS/IASME Int. Conf. on System Science and Simulation in Engineering, Tenerife, Spain, December 16-18, 2005 (pp186-191)

To compare the accuracy of robot before and after calibration, the absolute offset of two centers of gravity is examined and shown in Figs. 12 and 13 for each case.

Finally, the large value amount $r_{c.g.,c.w.}$ and $r_{c.g.,c.c.w.}$ as the measure of odometric accuracy for systematic errors is defined as:

$$E_{\max,sys} = \max\left(r_{c.g.,c.w.}; r_{c.g.,c.c.w.}\right) \tag{11}$$

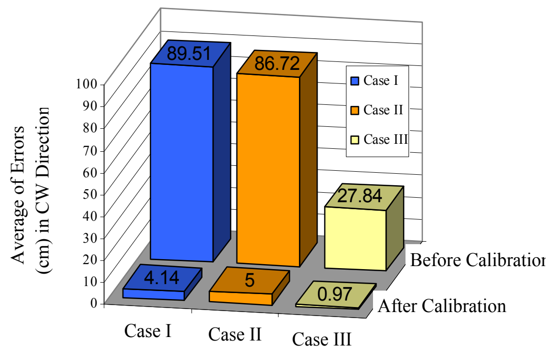


Fig. 12. Position of C.G for robot cases I, II and III in cw direction before and after calibration

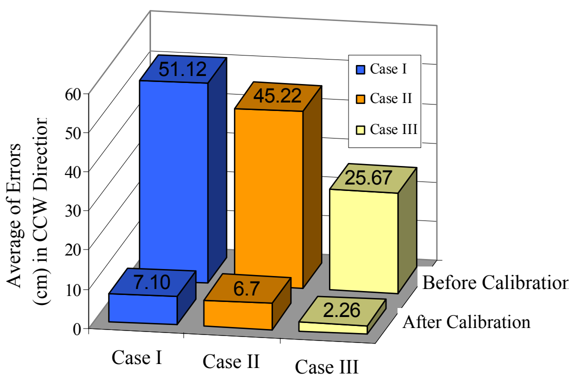


Fig. 13. Position of C.G for robot cases I, II and III in ccw direction before and after calibration

5 Statistical Analysis of Robot Tests Result

Performance comparison of robots can be achieved with the help of statistical investigation of test results. In effect, Normal distribution can be referred for analyzing the results. To be specific, the distance between robot final position and the origin, $e$ is derived using Eqs. (9) and (10). $\bar{e}$ the robot average error can be obtained as follows:

$$\bar{e} = \frac{\sum e}{n} \tag{12}$$

where n is the number of trials.

Using $d$ is difference and $\delta$ is standard derivation. The normal distribution curve is depicted using Eq. (13).

$$f(x) = \frac{1}{\delta\sqrt{2\pi}} e^{-0.5\left(\frac{x-\bar{e}}{\delta}\right)^2} \tag{13}$$

The normal distribution curve is delineated in cw and ccw directions using Eq. (13). The normal distribution curve of transitional error for Robotest is illustrated in Figures 14 and 15.

With the aim of investigating the convergence of robot final position in tests, the probability of final position being in a distance less than 3cm to centre of gravity of errors, is calculated. The forgoing calculations are undertaken for Robotest as shown in Fig. 16.

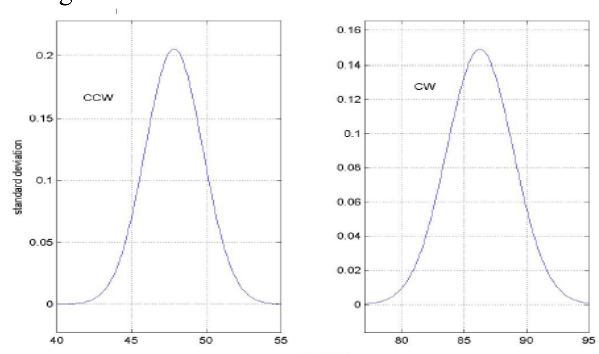


Fig. 14. The normal distribution curve of transitional error for Robotest before calibration

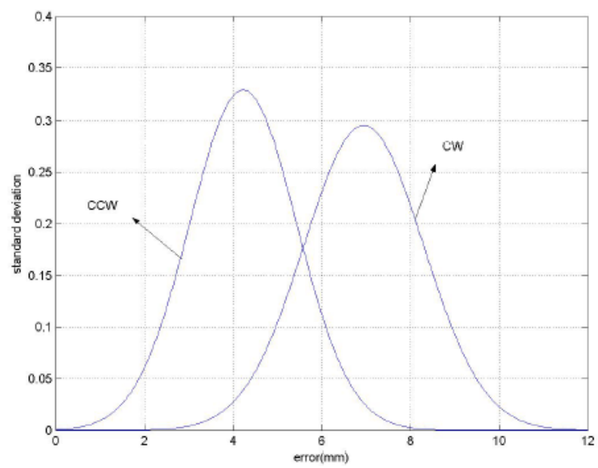


Fig. 15. The normal distribution curve of Robotest errors after calibration

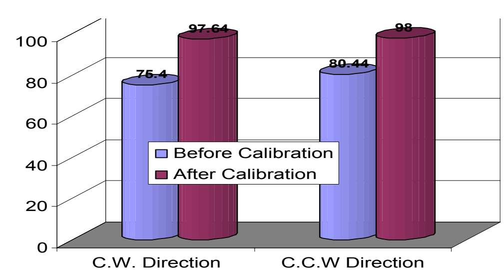


Fig. 16. Probability final position of Robotest motion being in a distance less than 3cm to C.G

The error distribution cure can be divided into three main regions:
1)The region between minimum and maximum occurred errors in trials.
2)The region defined between the zero error and minimum error.
3)The region defined as space with error greater than maximum error.
Considering above error distribution, the error occurrence probability in each zone before and after calibration for cw and ccw movements are calculated for all robots and that of Mobolab is demonstrated in Fig. 17. Performance monitoring of robots can be obtained as follows:

$$P_e = \frac{e_{BC} - e_{AC}}{e_{BC}} \tag{14}$$

Where $e_{BC}$ is maximum of error before calibration, $e_{AC}$ is maximum of error after calibration and $P_e$ is error decrease percentage.

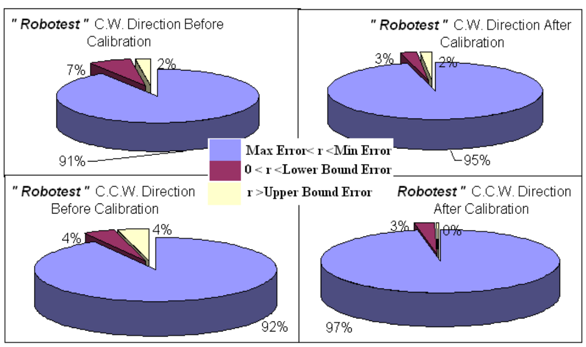


Fig. 17. The error occurrence probability in each zone before and after calibration for C.W. and C.C.W. movements for Mobolab

## 6 Conclusion

in this paper the design process of three differential drive robots were presented. To overcome the systematic errors, the Omni-Directional mobile robot was tested and moved in a different path. The experimental results showed the overall odometry accuracy of the robots. With choosing UMBmark method three differential drive robots tested and the systematic errors were modified and reduced by using the method. The absolute measurements of these errors are compared to the position and orientation of the robots as computed according to odometry data. After find the error sources, robots calibrated and tested again that result of tests presented.
Finally, four mobile robots test results analysis with using Normal Distribution and the Operation of each robot in difference state for two differential drive robots is presented. At the end comparison between robots Performance was presented.

## Reference

[1] Borenstein, J., Everett, H.R. and Feng, L., 1997, “Mobile robot positioning: Sensors and techniques”, J. Robot. Syst., vol. 14, pp. 231–249.
[2] Madahi Y. and Maddahi A, “Mobile Robots Experimental Analysis based on kinematics”, WSEAS Conferences, Turkey, 2004.
[3] Choi, B.J. and Sreenivasan, S.V., 1999, “Gross motion characteristics of articulated mobile robots with pure rolling capability on smooth uneven surfaces”, IEEE Trans. Robot. Automat., vol. 15, pp. 340–343.
[4] Hamdy, A. and Badreddin, E., 1992, “Dynamic modelling of a wheeled mobile robot for identification, navigation and control”, in Proc. IMACS Conf. Modeling and Control of Techno. Syst., pp. 119–128.
[5] Balakrishna, R. and Ghosal, A., 1995, “Modelling of slip for wheeled mobile robots”, IEEE Trans. Robot. Automat., vol. 11, pp. 126–132.
[6] Scheding, S., Dissanayake, G., Nebot, E.M. and Whyte, D.H., 1999, “Experiment in autonomous navigation of an underground mining vehicle”, IEEE Trans. Robot. Automat., vol. 15, pp. 85–95.
[7] Rajagopalan, R., 1997, “A generic kinematic formulation for wheeled mobile robots”, J. Robot. Syst., vol. 14, pp. 77–91.
[8]. Dickerson, S.L. and Lapin, B.D., 1991, “Control of an omni-directional robotic vehicle with mecanum